Design and Synthesis of 9,9-Dioctyl-9H-Fluorene Based Electrochromic Polymers

Qinglin Jiang, Shijie Zhen, Daize Mo, Kaiwen Lin, Shouli Ming, Zhipeng Wang, Congcong Liu, Jingkun Xu, Yuanyuan Yao, Xuemin Duan, Danhua Zhu, Hui Shi

Jiangxi Key Laboratory of Organic Chemistry, Jiangxi Science and Technology Normal University, Nanchang, 330013, People's Republic of China
Correspondence to: J. Xu (E-mail: xujingkun@tsinghua.org.cn)

ABSTRACT: Two novel heterocycle-fluorene-heterocycle monomers, 2,2′-(9,9-dioctyl-9H-fluorene-2,7-diyl)dithiophene (Th-F-Th) and 5,5′-(9,9-dioctyl-9H-fluorene-2,7-diyl)bis(2,3-dihydro-thieno[3,4-b][1,4]dioxine) (EDOT-F-EDOT), were synthesized via Stille coupling reaction and electropolymerized to form corresponding polymers P(Th-F-Th) and P(EDOT-F-EDOT). Furthermore, the optoelectronic properties of the obtained monomers and polymers were explored using cyclic voltammetry (CV), UV–vis, and emission spectra and *in situ* spectroelectrochemical techniques. The band gap values of monomers calculated by DFT were 3.75 eV for EDOT-F-EDOT and 4.03 eV for Th-F-Th, while that of P(EDOT-F-EDOT) and P(Th-F-Th) were brought down to 1.70 and 2.10 eV, respectively. Both polymers exhibited excellent redox activity and electrochromic performance. P(EDOT-F-EDOT) exhibited a maximum optical contrast of 25.8% at 500 nm in visible region with a response time of 1.2 s. In addition, the coloration efficiency of P(EDOT-F-EDOT) was calculated to be 220 cm^2 C^{-1}. © 2015 Wiley Periodicals, Inc. J. Polym. Sci., Part A: Polym. Chem. **2016**, *54*, 325–334

KEYWORDS: conducting polymers; copolymerization; electrochemical polymerization; electrochemistry; electrochromics; P(EDOT-F-EDOT); spectroelectrochemistry

INTRODUCTION Electrochromism is defined as a reversible change in absorbance/transmittance in response to an externally applied potential on a material.[1] Electrochromic (EC) materials have extensive applied prospects as intelligent materials, such as smart windows,[2] optical displays,[3] and electrochromic mirrors.[4] Conducting polymers (CPs) as electrochromic materials, since they were discovered, have attracted large number of attention due to outstanding coloration efficiencies, ease of color control through structure modification and fast switching ability.[5]

Among the numerous candidate CPs that have been studied, polythiophenes are a class of important EC materials because of high electrical conductivity, good redox behavior, and excellent electrochromic performance including fast response time and high contrast in the visible and NIR regions.[6] Also, polythiophenes exhibited facile bandgap tunability through structural modification, which has been proved by the reported novel materials in past few years.[7] In polythiophenes family, 3,4-ethylenedioxythiophene (EDOT) is the most common precursor used for electrochemical polymerization due to

electron-rich polymeric backbone possessing high oxygen content and inhibiting α, β- and β, β- cross-links.[8]

Polyfluorenes (PFs), due to excellent chemical and thermal stabilities, easy functionalization at the 9 positions and good fluorescence properties, have been used as electroactive materials.[9] Based on the advantages of PF and PEDOT, Nie et al.[9] have reported a kind of electrochromic polymer poly(2,7-bis(2,3-dihydrothieno[3,4-*b*][1,4]dioxin-5-yl)−9H-fluorene) (P(EDOT-FE)), a typical "poly(heterocycle-fluorene-heterocycle)" material, which showed a good electrochromic performance including good optical contrast (36% at 625 nm), high CE, fast response time (0.5 s at 625 nm), satisfactory optical memory and long-term stability. Furthermore, Önala and coworkers synthesized three new monomers based on furan and fluorene and investigated the optical properties of their corresponding polymers, which showed electrochromic properties and smaller band gap than PF (i.e., 3.1 eV).[10] Subsequently dozens of fluorene analogs based electrochromic polymers have been achieved (their structures are shown in Scheme 1), some of which displayed exceptional performance.

Qinglin Jiang, Shijie Zhen, and Daize Mo contributed equally to this manuscript.
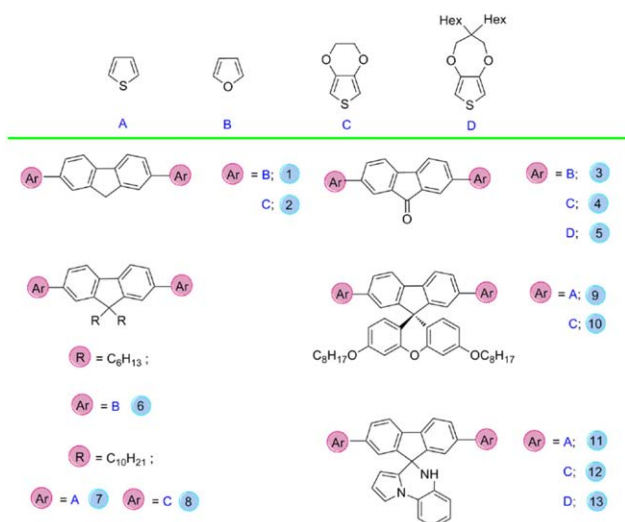
SCHEME 1 Structures of reported poly(heterocycle-fluorenes-heterocycle) electrochromic materials. [Color figure can be viewed in the online issue, which is available at wileyonlinelibrary.com.]

Although fluorene analogs based polymers exhibited good electrochromic properties, however, the poor solubility in common organic solvents limit their applications. One of the most promising ways to overcome these problems is to introduce alkyl chain structures at the bridge position of fluorene (C-9) position, which has been proved in previous work.[11] Substituents not only change the solubility of the system, but also affect the oxidation potential of monomer, the band gap and optical properties of the polymers. In addition, it was predicted that the alkyl substituted electrochromic polymer showed better contrast ratios and switching speeds than the parent polymer.[12–14]

According to these consideration, two novel heterocycle-fluorene-heterocycle monomers, Th-F-Th and EDOT-F-EDOT, were synthesized via Stille coupling reaction and electropolymerized to form corresponding polymers P(Th-F-Th) and P(EDOT-F-EDOT). In addition, electrochemical behavior, and electrochromic properties of the obtained polymers were systematically investigated by cyclic voltammetry (CV) and *in situ* spectroelectrochemical techniques. To elucidate the effect of the terminal group, the obtained results of EDOT-F-EDOT and corresponding polymer are compared with its close thiophene (Th) based analogues Th-F-Th and P(Th-F-Th).

EXPERIMENTAL

Chemicals
Thiophene (Th, 99%; TCI, Shanghai) and EDOT (98%; Sigma-Aldrich) were distilled under N_2 atmosphere once before

use. 9,9-Dioctyl-2,7-dibromofluorene (98%; J&K chemical), *n*-butyllithium (2.5 mol L^{-1} in hexanes; Energy Chemical), chlorotributyltin (98%; Energy Chemical) and tetrakis (triphenylphosphine) palladium (0) (99%; Energy Chemical) were stored at 4 °C and used directly without further purification. *N,N*-Dimethylformamide (DMF, analytical grade; Beijing East Longshun Chemical Plant) and dichloromethane (analytical grade; Beijing East Longshun Chemical Plant) were purified by distillation with calcium hydride under a nitrogen atmosphere before use. Tetrabutylammonium hexafluorophosphate (Bu_4NPF_6, 99%; Energy Chemical) was dried under vacuum at 60 °C for 24 h before use.
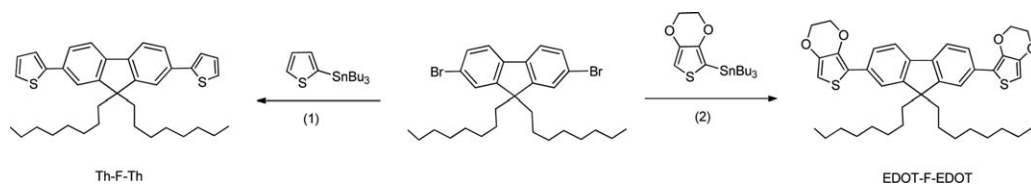
Monomer Synthesis
Two novel monomers, which comprise 9,9-dioctyl-2,7-dibromofluorene core symmetrically linked to Th and 3,4-ethoxylenedioxythiophene, namely 2,2′-(9,9-dioctyl-9H-fluorene-2,7-diyl)dithiophene (Th-F-Th) and 5,5′-(9,9-dioctyl- 9H-fluorene-2,7-diyl)bis(2,3-dihydrothieno[3,4-*b*][1,4]dioxine) (EDOT-F-EDOT), were prepared in satisfactory yield by the synthetic route in Scheme 2. In addition, the two monomers were synthesized and their properties were investigated for the first time as we known.

Tributyl(thiophen-2-Yl)stannane and Tributyl(2,3-dihydrothieno[3,4-*B*][1,4] dioxin-5-Yl)stannane
A solution of Th (or EDOT) in dry THF was cooled to −78 °C, and blanked by under an argon atmosphere.[15,16] *n*-BuLi (2.5 mol L^{-1} in hexane) was slowly added dropwise. The mixture was stirred for 1–2 h at −78 °C. Then a solution of chlorotributyltin in dry THF was added slowly at −40 °C, and the mixture was stirred for 2 h at the same temperature. After that, the reaction mixture was warmed to room temperature, and then was stirred for another 10 h under an inert atmosphere (Ar). The organic layer was dried with anhydrous $MgSO_4$ and filtered with funnel, and then the solvent was removed under reduced pressure by rotary evaporation. The stannic derivative was used without other purification for the Stille coupling reactions.

2,2′-(9,9-Dioctyl-9H-fluorene-2,7-diyl)dithiophene (Th-F-Th)
9,9-Dioctyl-2,7-dibromofluorene (0.5 g, 0.91 mmol) and tributyl(thiophen-2-yl)stannane (1.02 g, 2.73 mmol) were dissolved in dry DMF (40 ml) and tetrakis(triphenylphosphine) palladium (0) (100 mg, 0.091 mmol) was added under an inert atmosphere (Ar). The mixture was refluxed for 12 h at 100 °C under argon atmosphere (Ar). Then, the mixture was cooled to room temperature, with an equal amount of water poured into the flask, extracted with CH_2Cl_2, and washed

SCHEME 2 Synthetic route of monomers: (1) DMF, Pd(PPh$_3$)$_4$, 100 °C; (2) DMF, Pd(PPh$_3$)$_4$, 100 °C.

with saturated $NaHCO_3$ solution and water three times successively. The combined organic layer was dried over anhydrous $MgSO_4$ and concentrated under reduced pressure to leave a crude residue. Purification by chromatography on silica gel (EA:PE = 1:10) afforded 0.30 g Th-F-Th as a faint yellow liquid (60%). ^{1}H NMR (400 MHz, $CDCl_3$): δ 7.72 (d, $J = 8$ Hz, 1H), 7.64 (t, $J = 24$ Hz, 2H), 7.43 (d, $J = 4$ Hz, 1H), 7.33 (d, $J = 8$ Hz, 1H), 7.15 (t, $J = 8$ Hz, 1H), 2.06 (m, 2H), 1.11 (m, 10H), 0.83 (t, $J = 12$ Hz, 3H), 0.72 (s, 2H). Calcd for $C_{37}H_{46}S_2$: C, 80.14; H, 8.30; S, 11.55. Found: C, 80.05; H, 8.37; S, 11.58.

5,5′-(9,9-Dioctyl-9H-fluorene-2,7-diyl)bis(2,3-Dihydrothieno[3,4-B][1,4] dioxine) (EDOT-F-EDOT)

Synthesis of EDOT-F-EDOT was carried out in a similar manner as Th-F-Th under similar conditions. The reagents were 9,9-dioctyl-2,7-dibromofluorene (0.51 g, 0.91 mmol), tributyl(2,3-dihydrothieno[3, 4-b][1,4]dioxin-5-yl)stannane (1.22 g, 2.73 mmol) and tetrakis(triphenylphosphine) palladium(0) (0.1 g, 0.091 mmol). Yield: 64%; faint yellow solid (0.59 g). ^{1}H NMR (400 MHz, $CDCl_3$): δ 7.72 (d, $J = 8$ Hz, 1H), 7.64 (d, $J = 12$ Hz, 1H), 6.31 (s, 1H), 4.28 (d, $J = 28$ Hz, 4H), 1.98 (t, $J = 16$ Hz, 2H), 1.29 (t, $J = 28$ Hz, 5H), 1.09 (d, $J = 16$ Hz, 6H), 0.81 (d, $J = 4$ Hz, 3H), 0.78 (s, 2H). Calcd for $C_{41}H_{50}S_2O_4$: C, 73.43; H, 7.46; S, 9.55; O, 9.55. Found: C, 73.29; H, 7.57; S, 9.47; O, 9.67.

Electrosynthesis and Electrochemical Tests

All the electrochemical experiments and polymerization of the monomers were performed in a one-compartment cell with the use of Model 263A potentiostat-galvanostat (EG&G Princeton Applied Research) under computer control. For electrochemical tests, the working and counter electrodes were both Pt wires with a diameter of 0.1 mm, respectively. To obtain a sufficient amount of the polymer films for characterization, Pt sheet, or ITO-coated glass were employed as the working electrode and another Pt sheet was used as the counter electrode. They were placed 5 mm apart during the examinations. Prior to each experiment, these electrodes mentioned above were carefully polished with 1500 mesh abrasive paper (for ITO: immersed in ethanol for 6 h and then cleaned by ultrasonically wave for 15 min), cleaned successively with water and acetone, and then dried in air. An Ag/AgCl electrode directly immersed in the solution served as the reference electrode, with its electrode potential calibrated against a saturated calomel electrode, and it revealed sufficient stability during the experiments. All the solutions were deaerated by a dry nitrogen stream and maintained under a slight overpressure through all the experiments to avoid the effect of oxygen.

The polymer films were grown potentiostatically at the optimized potential in CH_2Cl_2 containing 0.1 mol L^{-1} Bu_4NPF_6 as the supporting electrolyte. After polymerization, the polymer films were washed repeatedly with anhydrous CH_2Cl_2 to remove the electrolyte, monomer, and oligomer.
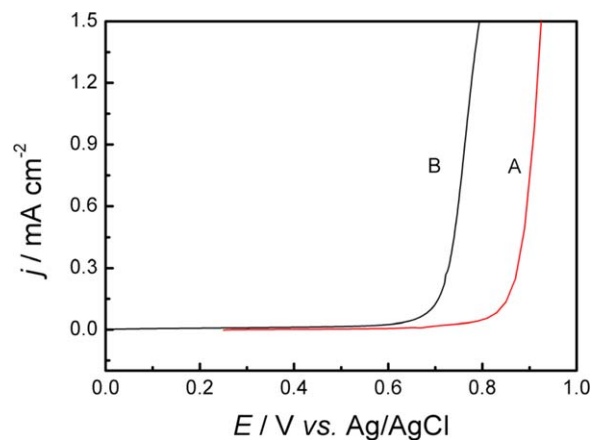

FIGURE 1 Anodic polarization curves of 0.01 mol L^{-1} Th-F-Th (A) and EDOT-F-EDOT (B) in CH_2Cl_2-Bu_4NPF_6 (0.1 mol L^{-1}). Potential scan rates: 50 mV s^{-1}. [Color figure can be viewed in the online issue, which is available at wileyonlinelibrary.com.]

Characterization

^{1}H NMR and ^{13}C NMR spectra were recorded on a Bruker AV 400 NMR spectrometer with $CDCl_3$ or DMSO-d_6 as the solvent and tetramethylsilane as an internal standard (TMS, singlet, chemical shift: 0.0 ppm). UV–vis spectra of the monomers and polymers were taken by using Cary 5000 UV–vis-NIR spectrophotometer. With an F-4500 fluorescence spectrophotometer (Hitachi), the fluorescence spectra of the monomers were determined. Infrared spectra were determined with a Bruker Vertex 70 Fourier transform infrared (FTIR) spectrometer with samples in KBr pellets. Electrochemical tests and polymerization of the monomers were performed in a one-compartment cell with the use of Model 263A potentiostat-galvanostat (EG&G Princeton Applied Research) under computer control. The surface morphology was captured in tapping mode by atomic force microscopy (AFM, Veeco Multimode). Spectroelectrochemical and kinetic studies were recorded on a Specord 200 Plus (Analytikjena) spectrophotometer at a scan rate of 2000 nm min^{-1} and the potentials were controlled using Versa Stat 3 (Princeton Applied Research) electrochemical workstation.

Electrosynthesis and Electrochemical Tests

Spectroelectrochemistry was recorded on a Specord 200 Plus (Analytikjena) spectrophotometer at a scan rate of 2000 nm min^{-1}. A three-electrode quartz cell was utilized consisting of an Ag/AgCl electrode, a Pt wire counter electrode, and an ITO coated glass working electrode. All measurements were carried out in CH_2Cl_2-Bu_4NPF_6 (0.1 mol L^{-1}). It should be noted here that the quartz cell filled with CH_2Cl_2-Bu_4NPF_6 (0.1 mol L^{-1}) and ITO-coated glass without deposited film were used as the background for spectroelectrochemical measurements.

The optical density ($\triangle$OD) at the specific wavelength (λ_{max}) of the sample was determined by %T values of electrochemically oxidized and reduced films, using the following equation[17]:
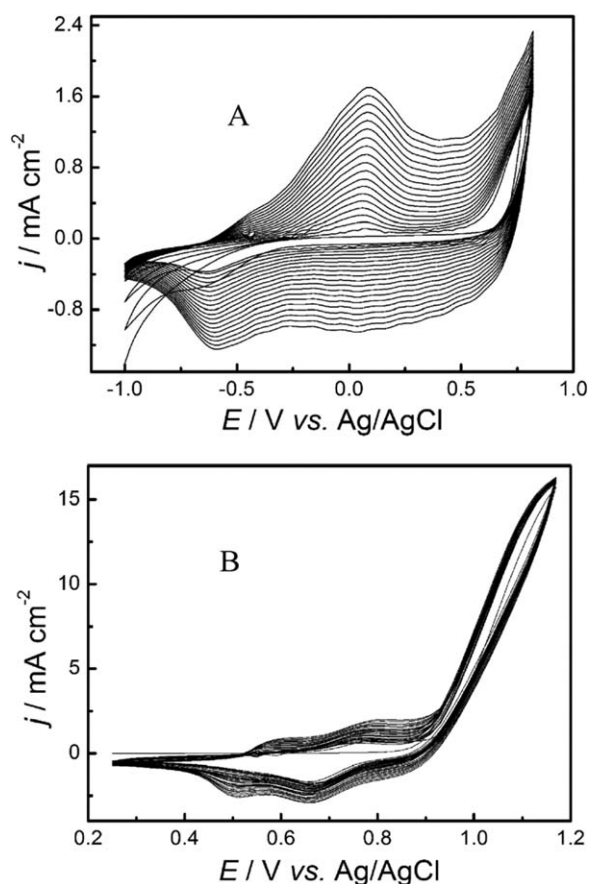
FIGURE 2 CV of 0.01 mol L^{-1} EDOT-F-EDOT (A) and Th-F-Th (B) in CH$_2$Cl$_2$-Bu$_4$NPF$_6$ (0.1 mol L^{-1}). Potential scan rates: 100 mV s^{-1}.

$$\Delta OD = \log(T_{ox}/T_{ref}) \tag{1}$$

The CE is defined as the relation between the injected/ejected charge as a function of electrode area (Q_d) and the change in optical density ($\triangle$OD) at the specific dominant wavelength (λ_{max}) of the sample as illustrated by the following equation[17]:

$$CE = \Delta OD/Q_d \tag{2}$$

The doping charge Q_d is defined as the relation between the injected/ejected charge during the redox process ($\triangle$Q) and working electrode area (S) at the specific dominant wavelength (λ_{max}) of the sample as illustrated by the following equation[17,18]:

$$Q_d = \Delta Q/S \tag{3}$$

$\triangle$Q can be directly obtained from the charge-time (C-t) curves, which conversed from the potential-time (E-t) curves directly recorded during the electrochromic experiments. S can be calculated by the area of the polymer films deposited onto the ITO glass.

Details of Computations

All calculations were carried out using the Gaussian 03 program. The structure of the oligomers were optimized without symmetry constraints using a hybrid density functional[19,20] and Becke's three-parameter exchange functional combined with the LYP correlation functional (B3LYP)[21,22] using the 6-31G(d,p) basis set (B3LYP/6-31G(d,p)). Vibrational frequencies were evaluated at the same level to identify the real minimum energy structures.

RESULTS AND DISCUSSION

Anodic Polarization Curves

Figure 1 shows the anodic polarization curves of 0.01 mol L^{-1} monomers (EDOT-F-EDOT and Th-F-Th) in CH$_2$Cl$_2$-Bu$_4$NPF$_6$ (0.1 mol L^{-1}). The oxidation of Th-F-Th and EDOT-F-EDOT were initiated at 0.87 and 0.71 V vs. Ag/AgCl, respectively. The difference between the onset oxidation potentials of two monomers was mainly due to electron-rich polymeric backbone possessing high oxygen content and inhibiting α, β- and β, β- cross-links.[23] However, these values are much lower than fluorene (1.05 V)[24], EDOT (1.2 V),[25] and Th (2.0 V),[26] which could be attributed to the increase of π-conjugated systems.[27] The method employing EDOT as the terminal groups presents an effective way to reduce oxidation potential of monomer.
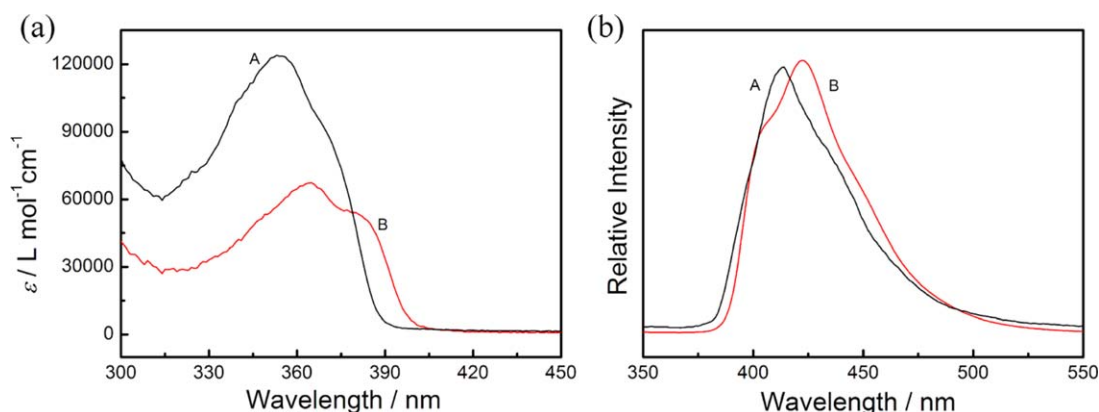

FIGURE 3 UV–vis spectra (a) and emission spectra (b) of Th-F-Th (A) and EDOT-F-EDOT (B) in CH$_2$Cl$_2$. [Color figure can be viewed in the online issue, which is available at wileyonlinelibrary.com.]

TABLE 1 Optical Data of EDOT-F-EDOT and Th-F-Th

Samples	λ (nm)	ε (L mol^{-1} cm^{-1})
EDOT-F-EDOT	368	67,000
	380	54,000
Th-F-Th	358	124,000
	367	97,000

ε is the absorption coefficient.

Cyclic Voltammetry

The electrochemical performances of two monomers were examined by CV in CH$_2$Cl$_2$-Bu$_4$NPF$_6$ (0.1 mol L^{-1}), as shown in Figure 2. The formation of this loop [Fig. 2(A,B)] can be explained as characteristic of the nucleation process, and only appeared on the first cycle. As the CVs scan continued, the peak current of the redox system increased regularly, indicating that electroactive polymer was formed. Meanwhile, visual inspection during electrochemical experiments revealed the formation of compact and homogeneous polymers on the electrode surface. From the CVs results, both P(EDOT-F-EDOT) and P(Th-F-Th) exhibited broad redox waves. The phenomenon usually appears in electrochemical behavior of Th/EDOT-based compounds,[28,29] and could be ascribed to the wide distribution of the conjugated polymer chain length and the mutual transition of multiple conductive species during the electropolymerization. In addition, EDOT-F-EDOT [Fig. 2(B)] exhibited better electropolymerization performances, which might be attributed to the electron-donating ethylenedioxy group and less structural defects.[18,23] It was noted that the alkyl chain substituents led P(EDOT-F-EDOT) film to exhibit sharper redox peaks than the parent P(EDOT-FE) film, which could be ascribed to the separation between polymer chains due to existence of alkyl chain.

UV–vis and Fluorescence Spectra of Monomers

UV–vis spectra and the absorption coefficient data of two monomers in CH$_2$Cl$_2$ were carefully examined, as shown in Figure 3(A). EDOT-F-EDOT and Th-F-Th showed similar absorption in the region of 320–400 nm, which corresponded to a distinctive π-π* transition.[14,30,31] It was noted that Th-F-Th exhibited scarcely discernible vibronic couplings at 358 and 367 nm in its π-π* transition band. Like Th-F-Th, the UV–vis spectra of EDOT-F-EDOT showed obvious vibronic coupling at 368 and 382 nm in its absorption band. It was suggested that vibronic splitting about conjugated monomers correlate to the rigid structure.[14,31] Furthermore, the splitted

absorption spectra were generally observed in hybrid conjugated samples containing long side chain.[14,28,30,31]

As shown in Table 1, it was noted that the absorption peak of EDOT–F–EDOT (λ_{max} = 368 nm, ε = 67,000 L mol^{-1} cm^{-1}) shifted to longer wavelength with decreasing absorption coefficient compared with that of Th–F–Th (λ_{max} = 358 nm, ε = 124,000 L mol^{-1} cm^{-1}), which could be attributed to electron-donating ethylenedioxy group of EDOT. In addition, the optical band gap of monomer was calculated on the basis of the formula $E_g = 1240/\lambda_{onset}$, where λ_{onset} is the onset of π-π* transition. The values of the optical bandgap for EDOT–F–EDOT and Th–F–Th were 3.08 and 3.19 eV, respectively (Table 2). The results are again consistent with the more electron-donating ability of EDOT in conjugated block.

The fluorescence emission spectra of monomers in CH$_2$Cl$_2$ were carefully determined, as shown in Figure 3(B). In agreement with the UV–vis spectral results, the emission spectra displayed significant red shift when the terminal unit change from Th (λ_{em} = 412 nm) to EDOT (λ_{em} = 422 nm). The difference was mainly attributed to the electron-donating ethylenedioxy group as in the case of the shift in UV–vis spectra.[18,22]

Structural Characterization

FTIR spectra of the oligomers and the hybrid polymers (Fig. 4) were recorded to elucidate their structure and interpret the polymerization mechanism. In the functional group region, the peak at 3070 cm^{-1} of EDOT-F-EDOT, and the peak at 3109 cm^{-1} of Th-F-Th, is attributed to the =C—H vibration of Th rings. However, these peaks disappeared in the spectra of P(EDOT-F-EDOT) and P(Th-F-Th), indicating that EDOT-F-EDOT and Th-F-Th could be electropolymerized at α-position of EDOT and Th, respectively. In the fingerprint region, the peaks at 1208 cm^{-1} [Fig. 4(A)] and 1173 cm^{-1} [Fig. 4(B)] should be assigned to the =C—H in-plane deformation vibration of Th rings, and 883 cm^{-1} [Fig. 4(A)] and 908 cm^{-1} [Fig. 4(B)] results from out-of-plane deformation vibration. However, all these peaks disappear or weaken in FT-IR spectrum of the polymer, which further demonstrated that Th-F-Th and EDOT-F-EDOT were electropolymerized through α, α'-coupling of Th rings.

Computational Results

To obtain a further interpretation of monomers, including planar structure, HOMO−LUMO levels, and bandgap, density functional theory calculations have been performed (Table 2 and Fig. 5). As it is seen from Table 1 the HOMO energy levels of monomer increase from Th-F-Th (−5.22 eV) to EDOT-

TABLE 2 The Calculated and Experimental Parameters of Th-F-Th and EDOT-F-EDOT

Samples	λ_{abs} (nm)	λ_{em} (nm)	$E_{ox,onset}$ (V)	HOMO (eV)		LUMO (eV)		$E_{g,opt}$ (eV)	
				Exp	DFT	Exp	DFT	Exp	DFT
Th-F-Th	358	407	0.87	−5.67	−5.22	−2.48	−1.47	3.19	3.75
EDOT-F-EDOT	368	472	0.71	−5.51	−5.14	−2.43	−1.48	3.08	3.66

Exp: experimental parameters; DFT: the calculated parameters through density functional theory calculations.
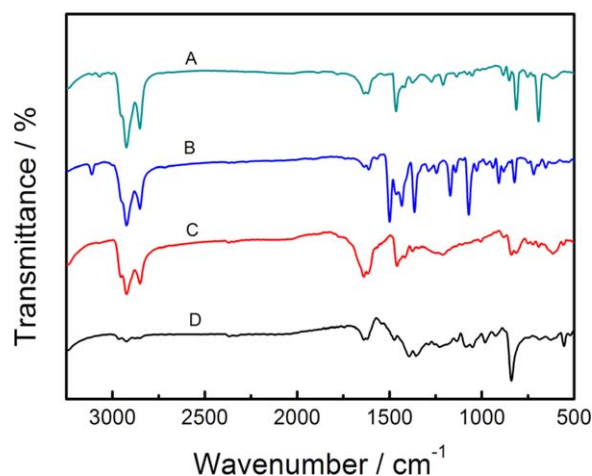
FIGURE 4 FTIR spectra of the oligomers and the hybrid polymers: (A) EDOT-F-EDOT, (B) Th-F-Th, (C) P(EDOT-F-EDOT), and (D) P(Th-F-Th). [Color figure can be viewed in the online issue, which is available at wileyonlinelibrary.com.]

FIGURE 5 HOMO and LUMO orbitals of monomers. [Color figure can be viewed in the online issue, which is available at wileyonlinelibrary.com.]

F-EDOT (-5.14 eV), which is in agreement with electron density of monomers. Compared with the change corresponding to HOMO of monomers, the difference of LUMO between Th-F-Th (-1.47 eV) and EDOT-F-EDOT (-1.48 eV) was found to be insignificant. In addition, the band gap of Th-F-Th and EDOT-F-EDOT, calculated on the basis of the for-
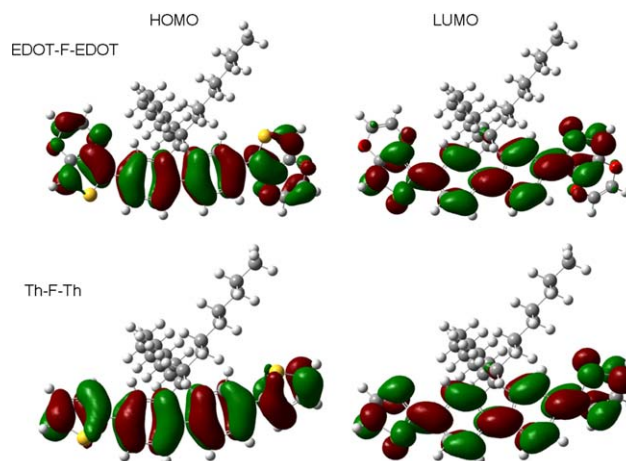
mula $E_g = $ LUMO-HOMO, were 4.03 and 3.75 eV, respectively. Furthermore, these values including HOMO, LUMO and band gap were found to be higher than those from experimental data, which could be explained by solvent effect.[15]

Electrochemistry of Polymer Films

To get a deeper insight into the electrochemical activity and stability of obtained polymers, the electrochemical behaviors
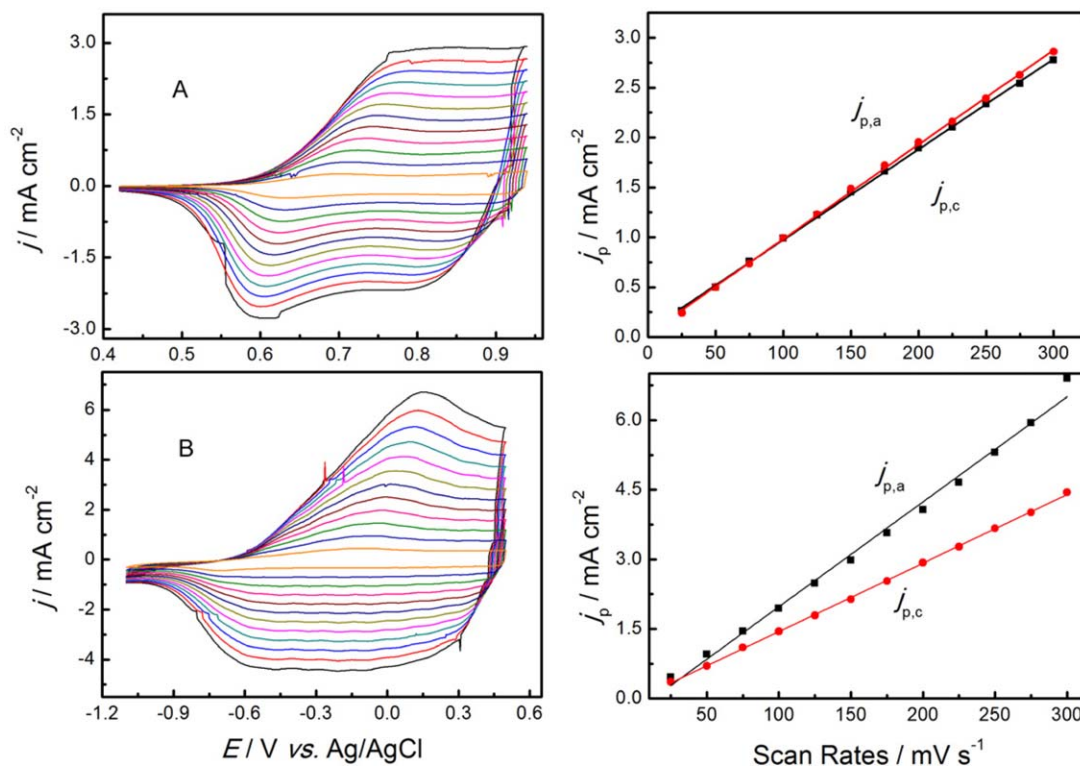

FIGURE 6 Left column: CV of P(Th-F-Th) (A) and P(EDOT-F-EDOT) (B) films in monomer-free CH_2Cl_2-Bu_4NPF_6 (0.1 mol L^{-1}) at potential scan rates of 25 mV s^{-1}, 50, 75, 100, 125, 150, 175, 200, 225, 250, 275, and 300 mV s^{-1}. Right column: plots of redox peak current densities versus potential scan rates. j_p is the peak current densities, and $j_{p,a}$ and $j_{p,c}$ denote the anodic and cathodic peak current densities. [Color figure can be viewed in the online issue, which is available at wileyonlinelibrary.com.]
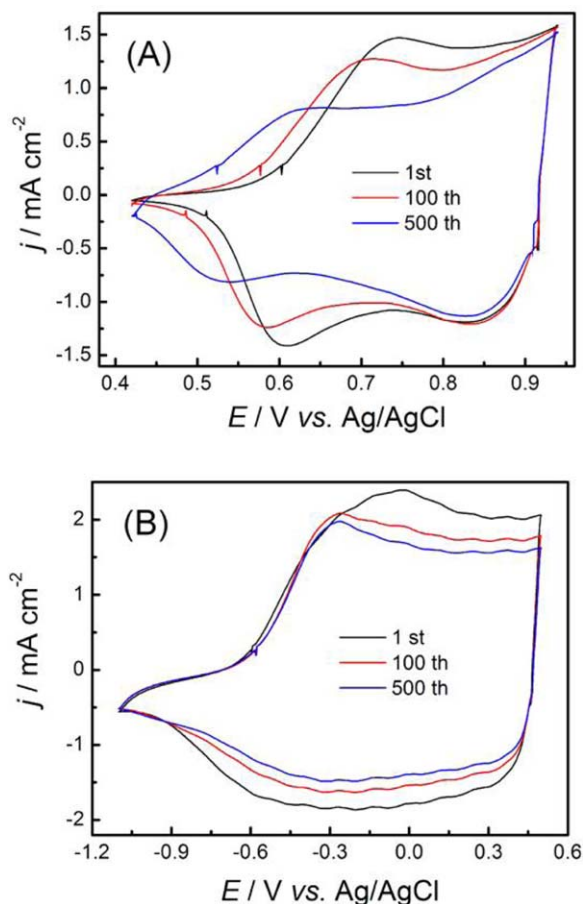
FIGURE 7 Long-term redox stability of P(Th-F-Th) (A) and P(EDOT-F-EDOT) (B) films in monomer-free CH_2Cl_2-Bu_4NPF_6 (0.1 mol L^{-1}) at the potential scan rate of 150 mV s^{-1}. [Color figure can be viewed in the online issue, which is available at wileyonlinelibrary.com.]

films or interfacial charge transfer process. In agreement with Figure 2, P(EDOT-F-EDOT) exhibited the sharper redox peaks the parent P(EDOT-FE) film. The result further demonstrated that the existence of alkyl chain facilitated better redox performance.

It is well known that the good stability of CPs is very significant for their applications in electronic devices.[33] Therefore, the long-term redox stability of two kinds of polymer films was also investigated in CH_2Cl_2-Bu_4NPF_6 (0.1 mol L^{-1}), as shown in Figure 7. It was noted that P(Th-F-Th) films exhibited better redox stability than P(EDOT-F-EDOT), retaining >89% of the electroactivity after 500 cycles, while P(EDOT-F-EDOT) displayed inferior redox activity with the amount of exchange charge remaining 79% after 500 cycles. In the literature EDOT based polymer generally exhibited superior stability than Th based polymer.[29,34−36] The exceptional stability of P(Th-F-Th) might be ascribed to narrower potential window compared with that of P(EDOT-F-EDOT) during redox process, as shown in Figure 6 (P(Th-F-Th) between −0.42 and 0.94 V; P(EDOT-F-EDOT) between −1.1 and 0.5 V).

of polymers were determined carefully by CV in monomer-free CH_2Cl_2-Bu_4NPF_6 (0.1 mol L^{-1}), as shown in Figure 6. The steady-state CVs of polymers represented broad anodic and cathodic peaks. The peak current densities, $j_{p,a}$ and $j_{p,c}$ (Fig. 6), were all proportional to the scan rate, which indicated that a reversible redox couple was fixed on the electrode and the electrochemical processes were non-diffusion controlled.[21] Furthermore, there is a stark difference between the anodic and cathodic peak potentials in CV curves, which due to hysteresis effect during redox process. The main reasons are usually as follows[32]: slow heterogeneous electron transfer, local rearrangement effect of polymer chains, slow mutual transformation of various electronic species, and electronic charging of interfacial exchange corresponding to the metal/polymer and polymer/solution interfaces, etc. Significantly, the driving voltages of P(EDOT-F-EDOT) was lower than that of P(Th-F-Th). The differences, corresponding with the highest occupied states in the valence band,[23] were commonly observed in the electrochemistry of CPs and may be due to a number of factors including the ease of diffusion of dopants in and out of the
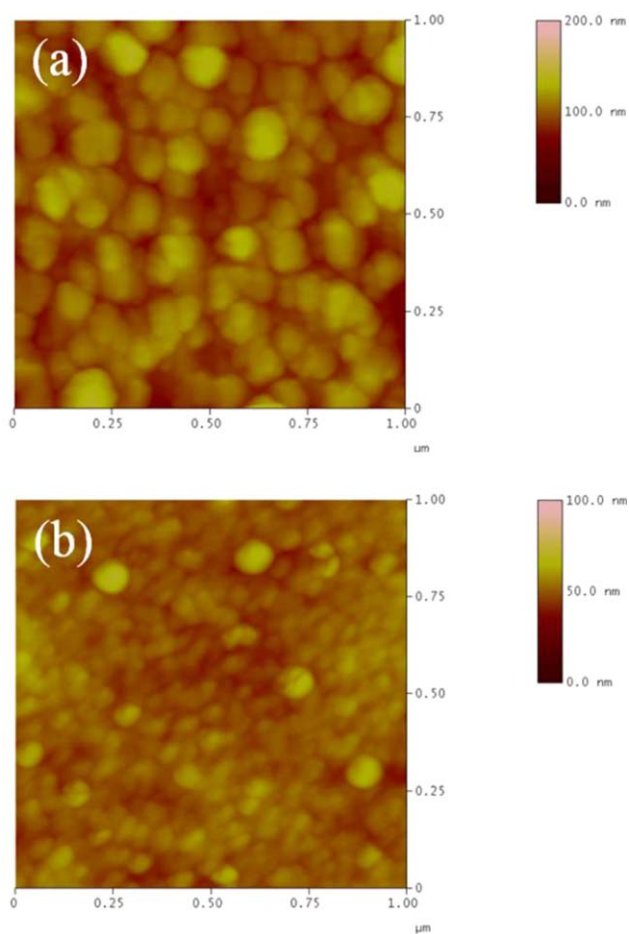

FIGURE 8 AFM images of P(Th-F-Th) (A) and P(EDOT-F-EDOT) (B) films deposited electrochemically on the ITO glass electrode. [Color figure can be viewed in the online issue, which is available at wileyonlinelibrary.com.]
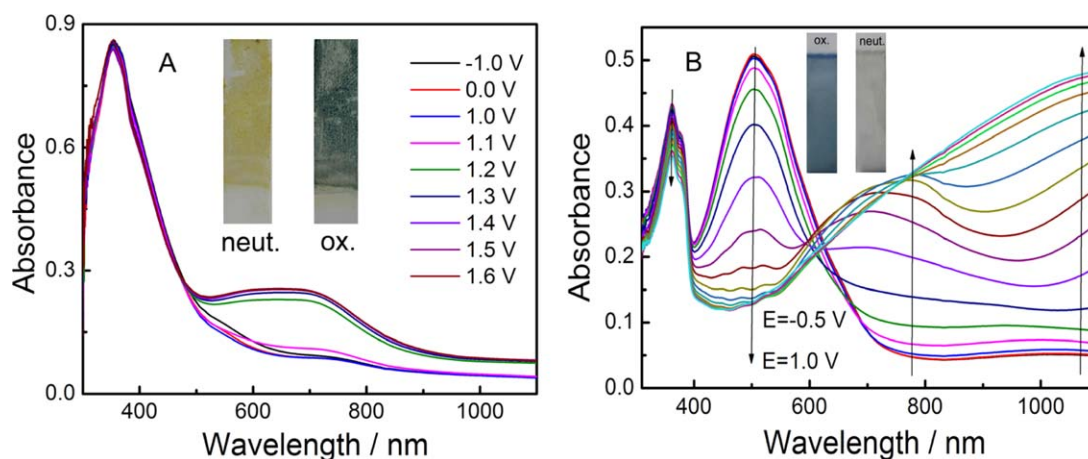
FIGURE 9 Spectroelectrochemistry for P(Th-F-Th) (A) and P(EDOT-F-EDOT) (B) electropolymerized on ITO coated glass in monomer-free CH_2Cl_2-Bu_4NPF_6 (0.1 mol L^{-1}). [Color figure can be viewed in the online issue, which is available at wileyonlinelibrary.com.]

Morphology

The surface morphologies of CPs are closely related to their properties, including electrical conductivity, redox activity, and stability, etc.[37] Therefore, the surface of the doped polymer films deposited electrochemically on the ITO electrode was observed by AFM images. As shown in Figure 8, the rms roughnesses of P(Th-F-Th) and P(EDOT-F-EDOT) were 12.60 and 4.23 nm, respectively, indicating that the morphology of P(EDOT-F-EDOT) was smoother than that of P(Th-F-Th).

Electrochromic Properties

Spectroelectrochemical and optical switching studies of these polymers were performed in monomer-free CH_2Cl_2-Bu_4NPF_6 (0.1 mol L^{-1}) to evaluate their electronic properties and band gaps and, consequently, to elucidate the function of the different terminal unit on the electronic properties of polymer films. As can be seen in Figure 9, P(EDOT-F-EDOT) revealed two well-defined absorption maxima at 364 and 500 nm in the neutral state; however, P(Th-F-Th) only shown one absorption band at 370 nm. It showed that the electron rich nature of EDOT resulted in a red shift in the spectrum. Furthermore, the absorption band of P(EDOT-F-EDOT) shifted to a longer wavelength of about 30 nm as compared to the analog P(EDOT-FE).[9] The result demonstrated that alkyl chain was beneficial to the increase of the conjugated block. Upon oxidation, P(EDOT-F-EDOT) showed the slightly fading of absorbance at 500 nm and typical evolution of peaks at more than 700 nm. Further oxidation, the absorption band at 775 nm began to decrease, whereas that in the NIR regime (1080 nm) increased, indicating the transition from polaron to bipolaron.[19]

As shown in Table 3, these changes of P(EDOT-F-EDOT) in the absorption spectra were accompanied with color changes from light gray ($L^* = 79$, $a^* = -5$, $b^* = -14$) to blue ($L^* = 70$, $a^* = 22$, $b^* = 0$) during doping process. Compared with P(EDOT-F-EDOT), P(Th-F-Th) showed unsatisfactory electrochromic property. As the applied potential increased, P(Th-F-Th) showed scarcely discernible absorption change at

370 nm. Fortunately, once the applied potential reached 1.2 V, the absorption band at 700 nm began to increase, which led to the color change from yellow ($L^* = 88$, $a^* = -4$, $b^* = 22$) to dark green ($L^* = 81$, $a^* = -12$, $b^* = 6$).

In addition, the optical band gap (E_g) of these polymers was calculated on the basis of the formula $E_g = 1240/\lambda_{onset}$, where λ_{onset} is the onset of π-π^* transition. The band gap of the P(Th-F-Th) was 2.1 eV, and the value was higher than that of P(EDOT-F-EDOT; 1.7 eV). Compared with P(EDOT-FE; $E_g = 1.96$ eV).

P(EDOT-F-EDOT) also revealed lower band gap, which could be ascribed to the longer conjugated block. However, the combination of EDOT and 9,9-dioctyl-9H-fluorene units under the same umbrella resulted in a hybrid compound, which has the intermediate band gap between PF (2.95 eV)[38] and PEDOT (1.61 eV).[23] It can be concluded that the band gap can be modified by incorporating Th/EDOT units into PF backbone.

The electrochromic parameters, such as optical contrast ratio ($\triangle T\%$) and response time are summarized in Table 4. The potentials were switching alternatively between reduced and oxidized states with residence time of 5 s.

TABLE 3 Colorimetric Data for Synthesized Polymers

Polymers		CIE color coordinates		Colors of polymers	
		Neutral	Oxidized	Neutral	Oxidized
P(Th-F-Th)	L^*	88	81		
	a^*	−4	−12		
	b^*	22	6		
P(EDOT-F-EDOT)	L^*	70	79		
	a^*	22	−5		
	b^*	0	−14		

TABLE 4 Electrochromic Parameters of P(EDOT-F-EDOT) and P(EDOT-FE)

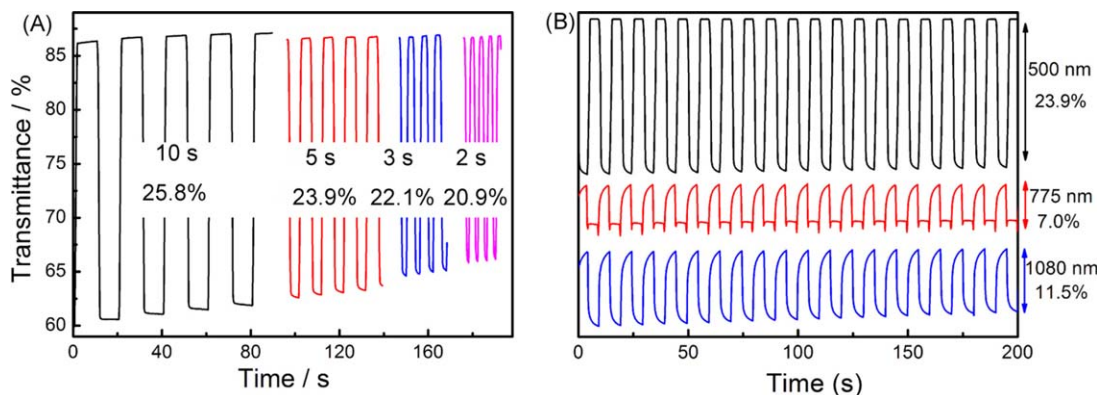| Polymers	λ (nm)	T_{red}	T_{ox}	ΔT	Response time (s)		CE (cm^2/C)	E_g (eV)
					Oxidation	Reduction		
P(EDOT-F-EDOT)	500	61.4%	87.2%	25.8%	1.2	1.6	220	1.70
	775	75.8%	68.8%	7.0%	0.6	3.8	22	
	1080	79.5%	68.0%	11.5%	2.6	3.4	106	
P(EDOT-FE)[9]	470	16%	41%	25%	1.6	1.0	415	1.96

FIGURE 10 Electrochromic switching: (A) P(EDOT-F-EDOT) was switched between -0.5 and 1.0 V with a switch time of 10, 5, 3, and 2 s at 500 nm; (B) optical absorbance change monitored for P(EDOT-F-EDOT) in monomer-free CH$_2$Cl$_2$-Bu$_4$NPF$_6$ (0.1 mol L^{-1}). Switching time: 5 s. [Color figure can be viewed in the online issue, which is available at wileyonlinelibrary.com.]

In the visible region (500 nm), P(EDOT-F-EDOT) showed 23.9% transmittance change between the neutral and oxidized states which was especially significant when considering the use in window- or display-type devices. The optical contrast was found to be 11.5% at 1080 nm. Herein, P(EDOT-F-EDOT exhibited similar electrochromic feature with P(EDOT-FE; Table 4), whereas superior than some analogs, such as poly(2,7-bis(2,3-dihydro-thieno[3,4-b][1,4]dioxin-5-yl)$-5'$H-spiro[fluorene-9,4$'$-pyrrolo [1,2-a]quinoxaline])(PEQE).[39] Unfortunately, the quality of the polymer P(Th-F-Th) film coated on ITO was not good, so it did not exhibit acceptable performance during polymer switching between its redox states. The polymer film is not stable and robust under ambient conditions and lost its electroactivity after a few cycles (Fig. 10).

Response time is an important parameter for a polymer since it indicates the speed of counter ions moving into and out of the polymer chains during the doping process. P(EDOT-F-EDOT) exhibited fast response time between neutral and oxidized state and achieved 95% of the optical contrasts within 0.6–3.8 s at all three wavelengths (Table 4). Especially, the response time during oxidation process was obvious faster than that of P(EDOT-FE) (1.6 s).[9] It was noted that the response time during oxidation was faster than the reduction process, which could be ascribed to the difference in charge transport rates between the two processes.

CE, calculated on the basis of the following formulas $\Delta OD = \log(T_{ox}/T_{red})$ and $CE = \Delta OD/Q_d$, is also a significant

criterion for identifying the performance of electrochromic material. CE of P(EDOT-F-EDOT) were calculated as 220 cm^2 C^{-1} (at 500 nm) and 106 cm^2 C^{-1} (at 1080 nm), respectively (Table 4). The value was apparent inferior than that of its analog P(EDOT-FE), whereas superior than that of poly(heterocycle-fluorenes-heterocycle) electrochromic materials including PEQE and poly(2,7-di(thiophen-2-yl)$-5'$H-spiro[fluorene-9,4$'$-pyrrolo[1,2-a]quinoxaline]) (PTQT).[39]

In addition, the optical stability was controlled by using a square wave potential step method together with measuring its spectra. The optical activity obtained after 100 cycles of
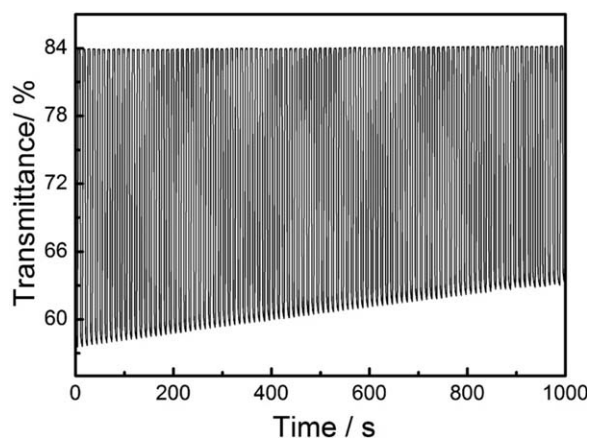

FIGURE 11 Optical stability at 431 nm between -0.5 and 1.0 V.

operation were found to be 80.7% of the starting activity (Fig. 11), in good agreement with CV results (87.2% after 100 cycles).

CONCLUSIONS

In summary, the synthesis and electrochemical polymerization of two heterocycle-fluorene-heterocycle monomers (Th-F-Th and EDOT-F-EDOT) were comprehensively reported. Structure-property relationships between P(Th-F-Th) and P(EDOT-F-EDOT), including optical property, surface morphology, electrochemical, and electrochromic performance, were comparatively investigated. Based on electrochemical result, the method employing Th/EDOT as the terminal groups presents an effective way to reduce oxidation potential of monomer. Meanwhile, P(EDOT-F-EDOT) revealed good electrochemical behavior and favorable electrochromic performance, such as fast response time (0.6 s) and high CE (220 cm^2/C).

ACKNOWLEDGMENTS

REFERENCES AND NOTES

1 Y. J. Tao, Z. Y. Zhang, X. Q. Xu, Y. J. Zhou, H. F. Cheng, W. W. Zheng, *Electrochim. Acta.* **2012**, *77*, 157–162.

2 A. Azens, C. G. Granqvist, *J. Electroanal. Chem.* **2003**, *7*, 64–68.

3 R. J. Mortimer, A. L. Dyer, J. R. Reynolds, *Displays* **2006**, *27*, 2–18.

4 M. E. Nicho, H. Hu, C. Lőpez-Mata, J. Escalante, *Sol. Energy Mater. Sol. Cells* **2004**, *82*, 105–118.

5 G. Sonmez, H. Meng, F. Wudl, *Chem. Mater.* **2004**, *16*, 574–580.

6 G. Sonmez, C. K. F. Shen, Y. Rubin, F. Wudl, *Angew. Chem. Int. Ed.* **2004**, *43*, 1498–1502.

7 C. Pozo-Gonzalo, M. Salsamendi, J. A. Pomposo, H. J. Grande, E. Y. Schmidt, Y. Y. Rusakov, B. A. Trofimov, *Macromolecules* **2008**, *41*, 6886–6894.

8 J. R. Reynolds, A. R. Katritzky, J. Soloducho, S. Belyakov, G. Sotzing, M. Pyo, *Macromolecules* **1994**, *27*, 7225–7227.

9 G. M. Nie, H. J. Yang, J. Chen, Z. M. Bai, *Org. Electron.* **2012**, *13*, 2167–2176.

10 A. Günes, A. Cihanerb, A. M. Önala, *Electrochim. Acta.* **2013**, *89*, 339–345.

11 S. Inaoka, R. Advincula, *Macromolecules* **2002**, *35*, 2426–2428.

12 L. B. Groenendaal, G. Zotti, P. H. Aubert, S. M. Waybright, J. R. Reynolds, *Adv. Mater.* **2003**, *15*, 855–879.

13 L. Beverina, G. A. Pagani, M. Sassi, *Chem. Commun.* **2014**, *50*, 5413–5430.

14 M. Li, Y. Sheynin, A. Patra, M. Bendikov, *Chem. Mater.* **2009**, *21*, 2482–2488.

15 G. E. Gunbas, A. Durmus, L. Toppare, *Adv. Mater.* **2008**, *20*, 691–695.

16 S. S. Zhu, T. M. Swager, *J. Am. Chem. Soc.* **1997**, *119*, 12568–12577.

17 C. L. Gaupp, D. M. Welsh, R. D. Rauh, J. R. Reynolds, *Chem. Mater.* **2002**, *14*, 3964–3970.

18 P. M. Beaujuge, J. R. Reynolds. *Chem. Rev.* **2010**, *110*, 268–320.

19 R. G. Parr, W. Yang, Density-functional Theory of Atoms and Molecules; Oxford University Press: New York, **1989**.

20 W. Koch, M. C. Holthausen, A Chemist's Guide to Density Functional Theory; Wiley-VCH: New York, **2000**.

21 C. Lee, W. Yang, R. G. Parr, *Phys. Rev. B.* **1988**, *37*, 785–789.

22 A. D. Becke, *J. Chem. Phys.* **1993**, *98*, 5648–5652.

23 A. Elschner, S. Kirchmeyer, W. Lvenich, U. Merker, K. Reuter, PEDOT: Principles and application of an intrinsically conductive polymer; Taylor & Francis Group: Boca Raton, **2011**.

24 M. Redecker, D. D. C. Bradley, M. Inbasekaran, E. P. Woo, *Appl. Phys. Lett.* **1998**, *73*, 1565–1567.

25 R. R. Yue, B. Y. Lu, J. K. Xu, S. Chen, C. C. Liu, *Polym. J.* **2011**, *43*, 531–539.

26 J. Roncali, F. Garnier, *Synth. Met.* **1986**, *15*, 323–331.

27 S. M. Zhang, J. K. Xu, B. Y. Lu, L. Q. Qin, L. Zhang, S. J. Zhen, D. Z. Mo, *J. Polym. Sci. Part A: Polym. Chem.* **2014**, *52*, 1989–1999.

28 B. Y. Lu, S. J. Zhen, S. M. Zhang, J. K. Xu, G. Q. Zhao, *Polym. Chem.* **2014**, *5*, 4896–4908.

29 K. W. Lin, S. L. Ming, S. J. Zhen, Y. Zhao, B. Y. Lu, J. K. Xu, *Polym. Chem.* **2015**, *6*, 4575–4587.

30 J. A. Kerszulis, K. E. Johnson, M. Kuepfert, D. Khoshabo, A. L. Dyer, J. R. Reynolds, *J. Mater. Chem. C.* **2015**, *3*, 3211–3218.

31 B. Karabay, L. Canan Pekel, A. Cihaner, *Macromolecules* **2015**, *48*, 1352–1357.

32 G. Inzelt, M. Pineri, J. W. Schultze, M. A. Vorotyntsev, *Electrochim. Acta.* **2000**, *45*, 2403–2421.

33 H. E. Katz, *Chem. Mater.* **2004**, *16*, 4748–4756.

34 K. W. Lin, S. J. Zhen, S. L. Ming, J. K. Xu, B. Y. Lu, *N. J. Chem.* **2015**, *39*, 2096–2105.

35 G. Q. Xu, J. S. Zhao, C. S. Cui, Y. F. Hou, Y. Kong, *Electrochim. Acta.* **2013**, *9*, 1125–1103.

36 X. J. Yang, M. Wang, J. S. Zhao, C. S. Cui, S. H. Wang, J. F. Liu, *J. Electroanal. Chem.* **2014**, *714715*, 1–10.

37 S. Beyazyildirim, P. Camurlu, D. Yilmaz, M. Gullu, L. Toppare, *J. Electroanal. Chem.* **2006**, *587*, 235–246.

38 P. Chen, G. Z. Yang, T. X. Liu, T. C. Li, M. Wang, W. Huang, *Polym. Int.* **2006**, *55*, 473–490.

39 A. Kivrak, B. B. Carbas, M. Zora, A. M. Önal, *React. Funct. Polym.* **2012**, *72*, 613–620.